Published in final edited form as:
Brain Res. 2013 January 15; 1490C: 117–127. doi:10.1016/j.brainres.2012.10.037.

Excitatory and inhibitory synaptic function in the rostral nucleus of the solitary tract in embryonic rat

Takeshi Suwabe[1], **Charlotte M. Mistretta**[1], and **Robert M. Bradley**[1,2]

[1]Department of Biologic and Materials Sciences, School of Dentistry, University of Michigan, Ann Arbor, MI 48109-1078

[2]Department of Molecular and Integrative Physiology, Medical School, University of Michigan, Ann Arbor, MI 48109-0622

Abstract

The embryonic development of synapses in the rostral nucleus of the solitary tract (rNST) was investigated in rat to determine when synapses begin to function. Using a brain slice preparation we studied appearance of synaptic receptors on second order rNST neurons and investigated the development of postsynaptic responses elicited by afferent nerve stimulation. Prenatal excitatory and inhibitory synaptic responses were recorded as early as E14. Glutamatergic and GABAergic postsynaptic responses were detected as early as E16. Both NMDA and AMPA receptors contributed to glutamatergic postsynaptic responses. GABAergic postsynaptic responses resulted primarily from activation of $GABA_A$ receptors. However, functional $GABA_C$ receptors were also demonstrated. A glycinergic postsynaptic response was not found although functional glycine receptors were demonstrated at E16. Solitary tract (ST) stimulation -evoked EPSCs, first detected at E16, were eliminated by glutamate receptor antagonists. ST-evoked IPSPs, also detected at E16, were eliminated by $GABA_A$ receptor antagonist. Thus, considerable prenatal development of rNST synaptic connections occurs and this will ensure postnatal function of central taste processing circuits.

Keywords

Taste; Solitary Tract Nucleus; Development; Brain slice; Electrophysiology

1. Introduction

The rostral nucleus of the solitary tract (rNST), the first relay in the central taste pathway, receives afferent projections from cranial nerves VII and IX that innervate taste receptors in the oral cavity. Central processes of the afferent taste fibers enter the lateral brainstem and establish the solitary tract (ST) that sends medially directed collateral branches to terminate in synapses with rNST neurons (King, 2006). Afferent synapses are located in clusters of nerve endings that contact dendritic processes but not the neuronal soma of second order neurons (Whitehead, 1986; Brining and Smith, 1996). A number of investigators have

Correspondence to: Robert M. Bradley, Department of Biologic and Materials Sciences, School of Dentistry, University of Michigan, Ann Arbor, MI 48109-1078, Phone: (734) 763-1080, FAX : (734) 647-2110, rmbrad@umich.edu.
Present address of Takeshi Suwabe: Department of Physiology, Osaka Dental University, Hirakata, Osaka 573-1121, Japan.

demonstrated that significant taste processing occurs at the rNST level of the central taste pathway in complex circuitry for sensory information within the brainstem, subsequently directed to the cortex (Smith and Lemon, 2006). Because newborns ingest milk and begin to sample food in the environment (Mistretta and Bradley, 1985), the rNST must be functional at birth. Thus, considerable prenatal development of rNST synaptic connections must occur to ensure postnatal function.

Previous electrophysiological investigations of the synaptic characteristics of adult rNST neurons have demonstrated a division into depolarizing excitatory postsynaptic potentials (EPSP), hyperpolarizing inhibitory postsynaptic potentials (IPSP) and a mixed EPSP and IPSP response (Wang and Bradley, 1995). Excitatory glutamatergic synapses are mediated by NMDA- and non-NMDA (AMPA/kainate)-type receptors in rNST (Wang, 1995). Application of the AMPA glutamate antagonist CNQX either reduces or blocks all EPSPs, and the NMDA receptor antagonist APV also reduces the amplitude of the EPSPs When both antagonists are applied, the EPSPs are entirely eliminated (Wang and Bradley, 1995). Furthermore, use of glutamate receptor antagonists *in vivo* results in the elimination of all taste evoked responses of rNST neurons (Li and Smith, 1997). In all, these results demonstrate that excitatory synapses between gustatory afferents and rNST neurons are glutamatergic, involving both AMPA and NMDA receptors.

Inhibitory activity in rNST has been studied by superfusing GABA agonists and antagonists over brain slices of the medulla while recording from rNST neurons. All rNTS neurons respond to GABA (Wang and Bradley, 1993; Du and Bradley, 1998), and use of the $GABA_A$ receptor agonist muscimol and antagonist bicuculline confirm that $GABA_A$ receptors are the predominant GABA receptor in rNST.

A time line for the emergence of these different types of synaptic activity is not known for rodent rNST. However, ion channel development has a widely ranging prenatal course and changing channel properties can contribute to emergence of synaptic properties and initial establishment of neural circuits in rNST neurons (Suwabe et al., 2011). NST synaptic thickenings appear at E15 and simple symmetrical membrane thickenings are seen at E17 followed by the appearance of vesicles at E19 (Zhang and Ashwell, 2001a). The sparse information on postnatal NST synapse maturation includes descriptions of transformations in the morphology of axon terminals (Rao et al., 1999), dendritic spines and filopodia (Vincent and Tell, 1999) and synaptic density (Lachamp et al., 2002). GABAergic synaptic density reportedly increases from E20 to P20 (Dufour et al., 2010; Yoshioka et al., 2006).

Understanding how and when rNST synapses begin to function during embryonic development is a necessary first step for any future studies about regulatory factors in the formation of rNST circuits involved in taste processing. Also, because a remarkable plasticity is documented in the postnatal taste system (Hill and May, 2006), study of temporal events in development of rNST function is necessary to understand the biological underpinnings and limitations of taste plasticity. In the current study we investigated the development of synaptic function of rNST neurons in prenatal rodents detailing both electrophysiological and pharmacological properties during a broad gestational period.

2. Results

2.1. Location of the recording sites

Neuron location was confirmed in calbindin and neurofilament immunoreacted slices after recording (three embryos each at E16, E18 and E20). Lucifer yellow stained, recorded neurons were observed among calbindin-immunopositive neurons (Fig. 1A, A', B, B') demonstrating that recording sites were located in the presumptive rNST. With

neurofilament immunoreactions (three embryos each at E16, E18 and E20) we defined the relationship of neurons to the developing ST. As shown in Fig. 1C, C', D, D', the Lucifer yellow filled neurons are located medial to the ST in a meshwork of neurofilament stained fibers that appear to be collateral branches of the ST. Again this places recorded neurons in the area of the presumptive rNST.

2.2. Passive membrane properties

Included in data analysis were 93 neurons, with an average V_{rest} of −46 ± 1 mV; R_{input} 2.4 ± 0.1 MΩ; membrane time constant 82 ± 4 ms; and, membrane capacitance 35 ± 1 pF. These values are within the range of basic neuronal characteristics that we reported for embryonic rNST neurons (Suwabe et al., 2011). We note embryo age and numbers of neurons throughout the results.

We studied embryonic synapse properties with two broad approaches: (1) to identify synaptic receptor types in rNST neurons and, (2) to characterize postsynaptic potentials elicited by ST stimulation. Results are organized to present excitatory and inhibitory synaptic properties.

2.3. Synaptic receptor expression in prenatal rNST neurons

2.3.1. Excitatory receptor expression—rNST neurons at E14 respond to glutamate (0.5 mM) which depolarized V_m by 14 ± 0.3 mV in all E14 neurons tested (n = 5) (Fig. 2A). The presence of NMDA and AMPA/kainate glutamate receptors in prenatal rNST was determined by superfusion of 100 μM NMDA and 10 μM AMPA at E16 (n = 8) and E20 (n = 4). All neurons tested responded to NMDA and AMPA application by average membrane depolarization of 24 ± 3 mV and 30 ± 7 mV (Figs. 2B and 2C), respectively. Thus, glutamate is an excitatory neurotransmitter at E14 and both NMDA- and AMPA-type receptors are expressed and functional in rNST neurons as early as E16.

2.3.2. Inhibitory receptor expression—All E14 neurons tested (n = 5) (Fig. 3A) also respond to 0.5 mM GABA which hyperpolarized the neurons by 35 ± 3 mV. These changes in V_m were associated with reductions of V_m responses to hyperpolarizing current pulses indicating reductions of R_{input}. Thus, rNST neurons express GABA receptors as early as E14.

GABA receptors are of three subtypes, $GABA_A$, $GABA_B$ and $GABA_C$. $GABA_A$ and $GABA_B$ receptors have been shown to be involved in inhibitory synapses in adult rNST (Wang and Bradley, 1995). To test for expression of GABA receptors in prenatal rNST neurons, we recorded responses to the $GABA_A$ receptor agonist muscimol and $GABA_B$ receptor agonist baclofen at E16 (n = 7) and E20 (n = 10).

The $GABA_A$ agonist, 10 μM muscimol, hyperpolarized V_m by 16 ± 1 mV with a reduction of V_m (Fig. 3B). In contrast, none of the neurons that responded to muscimol responded to 100 μM baclofen (Fig. 3C). We used a higher concentration (1 mM) of baclofen in neurons at E18 (n = 5), but none of the neurons showed significant response to baclofen. All of these neurons were hyperpolarized by 0.5 mM GABA that was applied after washout (> 20 min) of baclofen. These results indicate that whereas $GABA_A$ receptors are functional in embryonic rNST neurons (muscimol effects), neural responses to GABA via $GABA_B$ receptor were not discernible in prenatal rNST neurons. However, we found that baclofen hyperpolarized V_m in rNST neurons at postnatal (P) day 40 (n = 5) confirming a previous report of $GABA_B$ receptor activity in adult rNST (Wang and Bradley, 1995).

$GABA_C$-receptor-mediated responses have been reported in early postnatal neurons between P0 and P14 but not after P21 (Grabauskas and Bradley, 2001). In investigating the expression of $GABA_C$ receptors in prenatal rNST neurons that responded to GABA, we recorded GABA-induced hyperpolarization in the presence of the $GABA_A$ receptor antagonist bicuculline (BMI) at E16 ($n = 5$) and E20 ($n = 5$). At high concentrations (100 or 200 μM) BMI reduced the amplitude of the hyperpolarization induced by 1 mM GABA application (Fig. 4A). Because we have already demonstrated that $GABA_B$-receptor-mediated neural response was negligible in prenatal rNST neurons, the BMI-insensitive hyperpolarization must represent $GABA_C$ receptor activity. Furthermore, as shown in Fig. 4B, the decay of GABA-induced hyperpolarization was slower in the presence of BMI (48% and 6% decay 10 s after the peak in the absence and presence of BMI respectively) indicating that desensitization to GABA was weaker in the presence of BMI. Insensitivity to BMI and relatively weak desensitization to GABA are established characteristics of $GABA_C$ receptor activity (reviewed in Bormann and Feigenspan, 1995).

Glycine is a major inhibitory synaptic transmitter in rat brainstem including the NST (Batten et al., 2010; Dufour et al., 2010a; Dufour et al., 2010b; Rampon et al., 1996; Zafra et al., 1995). We tested expression of glycine receptors in prenatal rNST neurons ($n = 10$ at E16) and found that 1 mM glycine hyperpolarized V_m by 15 ± 4 mV associated with reduction of V_m responses to hyperpolarizing current pulses (Fig. 5). The data indicate that glycine receptors are expressed and functional as early as E16 in rNST neurons.

In all, we find evidence of GABA and glycine receptors in rNST as early as E16. Further, we demonstrated $GABA_A$ and $GABA_C$, but not $GABA_B$, function in embryonic rNST. $GABA_B$ receptor function is, however, documented in postnatal rNST (Wang and Bradley, 1995), with a distinctive developmental time course.

2.4. Postsynaptic responses evoked by ST current stimulation in prenatal rNST neurons

Having determined that glutamate, GABA and glycine receptors are functional in embryonic rNST, we investigated the characteristics of prenatal postsynaptic responses by stimulation of the ST in rNST neurons at E16 ($n = 5$), E18 ($n = 2$) and E20 ($n = 2$). ST-evoked EPSCs were already detectable at E16. EPSCs, observed in voltage-clamp recordings (61 ± 3 pA; filled arrowhead in Fig. 6A), were eliminated by an AMPA/kainate receptor antagonist CNQX (10 μM) ($n = 9$; open arrowhead in Fig. 6B).

In a further set of neurons at E16 ($n = 5$) and E20 ($n = 5$), EPSPs were observed in current-clamp recordings (5 ± 2 mV; arrowhead in Fig. 7A) when slices were superfused with normal ACSF. The amplitude of EPSPs significantly increased (22 ± 5 mV; double arrowhead in Fig. 7B) when normal ACSF was replaced with Mg^{2+}-free ACSF. The enlarged EPSPs were significantly suppressed (5 ± 1 mV; open arrowhead in Fig. 7C) by an NMDA-type receptor antagonist APV (50 μM). The EPSP amplitude returned to prior levels after APV washout (double arrowhead in Fig. 7D). Thus, AMPA/kainate and NMDA receptor-mediated glutamatergic synapses are established as early as E16 in rNST, confirming data with superfused AMPA and NMDA in Fig. 2.

ST-evoked IPSPs were also detectable at E16. IPSPs were observed in current-clamp recordings ($n = 5$ at E16 and $n = 5$ at E20; Figs. 8A and 8C). These IPSPs were eliminated by 100 μM BMI alone (Figs. 8B and 8D) indicating that a GABAergic inhibitory neural network between the ST and rNST neurons was established by E16. It should be noted that no other IPSPs (e.g., $GABA_C$- or glycine-receptor-mediated IPSP) were observed during the application of BMI. The onset time of IPSPs largely varied with trials and single stimulation sometimes evoked multiple IPSPs (asterisks in Fig. 8C). These results suggest convergence of polysynaptic neural pathways to single rNST neurons. In a further group of rNST neurons

at E18 (n=5), IPSPs and EPSPs were eliminated by a mixture of 10 μM CNQX and 100 μM APV (data not shown) suggesting that polysynaptic inhibitory neural pathways involve glutamatergic synapses.

3. Discussion

We have demonstrated prenatal synaptic activity in the brainstem taste relay nucleus, rNST, and as early as E14 show that both excitatory (glutamate) and inhibitory (GABA) receptors are functional. Indeed, glutamatergic and GABAergic *postsynaptic responses* were detected as early as E16. As summarized in Fig. 9 both NMDA and non-NMDA (AMPA/kainate) receptors contributed to glutamatergic postsynaptic responses. Whereas GABAergic postsynaptic responses resulted primarily from activation of $GABA_A$ receptors, functional $GABA_C$ receptors were also demonstrated. A glycinergic postsynaptic response was not found although functional glycine receptors were demonstrated at E16. The data on embryonic rNST synapse activity paint an image of potentially complex function as brainstem taste circuits are emerging.

In rNST neurons, ST-evoked, $GABA_A$-receptor-mediated IPSPs were apparent as early as E16. The $GABA_A$-receptor-mediated IPSPs are also observed in early postnatal (Grabauskas and Bradley, 2001) and adult rNST neurons (Wang and Bradley, 1995). In contrast, $GABA_C$- and $GABA_B$-receptor-mediated postsynaptic responses emerge at different times. Whereas $GABA_C$ receptors are functional at E16 they do not contribute to evoked IPSPs. $GABA_C$- and $GABA_B$- receptor-mediated IPSPs are detected in early postnatal (P0 - 14) and adult rNST neurons respectively. This developmentally regulated emergence suggests the potential for different roles of GABA receptor subtypes in the development of the brainstem gustatory relay nucleus.

ST-evoked, glycinergic postsynaptic responses could not be recorded in prenatal rNST neurons. Similar observations have been reported in early postnatal and adult rNST neurons (Grabauskas and Bradley, 2001; Wang and Bradley, 1995). These data indicate that afferent fibers of ST do not drive glycinergic input to rNST neurons. However, because glycine receptors were functional as early as E16 in rNST neurons, glycinergic input may be driven from other neural pathways or glycine may be spontaneously released from presynaptic terminals (Dufour et al., 2010).

3.1. Anatomical development of rNST synapses

The developmental progression of synapse formation in rat rNST begins with production of geniculate (facial nerve) and petrosal ganglion (glossopharyngeal nerve) cells at E10 - E13 (Fig. 9). In classic anatomical data, central processes from the facial and glossopharyngeal ganglion neurons contribute to formation of the ST at E12 and E14 respectively (Altman and Bayer, 1982). Simultaneously, presumptive rNST neurons are produced between E10 and E13 with a peak at E12 (Altman and Bayer, 1980).

Synaptic connections from afferents to rNST neurons were described from E15, and synaptic vesicles merged at synaptic terminals by E18 (Zhang and Ashwell, 2001a). At E19, typical synaptic junctions are identified in all NST subnuclei (Zhang and Ashwell, 2001a).

We now have shown that by E14, rNST neurons are already excitable and express functional glutamate and GABA receptors. In the absence of detailed evidence for morphology of embryonic synapses and emerging circuitry, we are left with very basic knowledge of early taste afferents in the ST (E13-E15) and neurons in NST (E11-E14). Aspects of synapse development are indicated from E15-E19. Our results of synaptic activity from E14 fit

within the known anatomical constraints; however our functional data suggest that future studies may well identify synapses in rNST at earlier embryo stages.

Our data indicate that postsynaptic function, ST-evoked glutamatergic and GABAergic postsynaptic responses, is developed at E16 before the anatomical description of the establishment of 'mature' presynaptic structures at E19 (Zhang and Ashwell, 2001b). However, it is possible that additional morphological investigation will reveal a different developmental sequence more synchronized with the functional appearance of synaptic activity in rNST. Moreover, brainstem postsynaptic responses have been recorded when presynaptic structures are anatomically immature in the caudal nucleus of the solitary tract (Balland et al., 2006; Sato et al., 1998) and the trigeminal nuclear complex (Momose-Sato et al., 2004). In caudal NST excitatory synapses were identified first at E18 (Balland et al, 2006). Inhibitory axon terminals and synapses were noted from E20 (Dufour et al., 2010a). In the trigeminal complex, postsynaptic function is demonstrated as early as E14 well (Momose-Sato et al., 2004) in advance of apparent conventional synapses in morphological studies (E17 and E19) (Al-Ghoul and Miller, 1993). In rostral and caudal NST and the trigeminal complex, therefore, brainstem synaptic function is demonstrated before mature synaptic structures.

Responses in morphologically immature synapses might be a type of paracrine intercellular communication that has been reported in developing hippocampal neurons (Demarque et al., 2002). In this mechanism, neural transmission is mediated by glutamate and GABA released without synaptic vesicle formation. Various functional roles for embryonic synapse structures and activity should be considered as firm data continues to come forward for prenatal synapses in rNST.

3.2. Development of pre- and postsynaptic function

In the embryo glutamatergic postsynaptic responses are mediated by NMDA and non-NMDA receptors. GABAergic postsynaptic responses are mediated solely by $GABA_A$ receptors. Whereas $GABA_C$ and glycine receptors are already functional in embryonic rNST neurons, ST-evoked postsynaptic responses mediated by these receptors are not detectable. $GABA_C$-receptor-mediated postsynaptic responses appear in rNST neurons between P0 and P14.

Other investigators have reported a similar temporal development of neurotransmitter receptors that precedes the appearance of synaptic activity and have detailed how neurotransmitters have various roles in neural development (reviewed in Manent and Represa, 2007). Both glutamate and GABA have been shown to regulate neuron proliferation, growth, migration, differentiation and survival (Nguyen et al., 2001; Manent and Represa, 2007). NMDA and $GABA_{A/C}$ receptors can participate in influencing neuronal migration in cortical development (Behar et al., 1996; Kihara et al., 2002; Komuro and Rakic, 1993; Heck et al., 2007; Hirai et al., 1999). In developing mouse cerebellum, NMDA receptor block decreased the migratory distance before synapse formation (Komuro and Rakic, 1993). Thus, the early expression of glutamate and GABA receptors in rNST neurons suggests the potential for similar roles in proliferation, migration and differentiation of presumptive rNST neurons.

3.4. Possible influence of afferent activity on rNST synaptic development

Neurobiologists have long known that neural activity can refine the patterning of neural connections (Katz and Shatz, 1996). Glutamatergic synaptic activity influences neural network formation including axonal growth and sensory afferent projection patterns in the visual system (Herrmann and Shatz, 1995; Shatz and Stryker, 1988; Sretavan et al., 1988).

In the developing somatosensory system, activity in postsynaptic NMDA receptors plays an important role in organization of afferent input in the trigeminal somatosensory pathway (Iwasato et al., 1997; Schlaggar et al., 1993; Li et al., 1994).

It has been suggested that synaptic activity in rNST affects gustatory terminal field organization and synaptic connections (Mangold and Hill, 2007; May et al., 2008). Moreover, because development of the ascending gustatory pathway has been shown to take place sequentially from the periphery to the parabrachial nucleus (Hill et al., 1982; Hill et al., 1983; Hill, 1987; Lasiter and Kachele, 1988; Lasiter et al., 1989), synaptic connections and activity in rNST would influence development of neural circuits in higher gustatory relays.

Remarkably, dietary sodium restriction in the pregnant dam during early embryonic development influences the organization of primary gustatory afferents in rNST (Mangold and Hill, 2007). This restriction alters rNST neuron morphology (King and Hill, 1993) and the postnatal response magnitudes to lingual application of sodium (Vogt and Hill, 1993). This suggests that reduced synaptic activity between afferent fibers and rNST neurons influences the organization of gustatory afferent input, possibly by NMDA receptor-dependent refinement of synaptic connections (Iwasato et al., 1997).

3.5 Summary

Based on the results of the current investigation and published details of morphological development, a developmental time line of rNST formation has been summarized in Fig. 9. Cells of the geniculate and petrosal ganglia are produced between E10 - E13 with a peak at E12 (Altman and Bayer, 1982). Central processes of the geniculate ganglion enter the brainstem, turn caudally to form the ST between E13 and E15. Between E12 and E15 the presumptive neurons of rNST are produced (Altman and Bayer, 1982). Collateral processes of the ST begin to make contact with developing rNST neurons at E14 and by E18 have matured with synaptic vesicles and thickenings.

As early as E14, embryonic rNST neurons respond to application of glutamate and GABA. Use of glutamate and GABA receptor antagonists reveals that both NMDA and AMPA/kinate glutamate receptors are involved in embryonic glutamate responses and $GABA_A$ receptors predominate in GABA responses. $GABA_C$ responses were demonstrated in late embryonic ages, but $GABA_B$ responses were not demonstrated until after birth. From E16, postsynaptic responses could be evoked by stimulation of the ST. Both EPSPs and IPSPs were recorded, mediated by NMDA and non-NMDA receptors. Inhibitory responses were mediated by activation of $GABA_A$ receptors. Although glycine responses were elicited via direct application to the recorded neurons, postsynaptic responses mediated by glycine were not observed. Postsynaptic responses attributable to GABAC receptors did not appear until P0.

The summary of known time courses for ganglion, tract and neuron development, with rNST neuron formation and acquisition of synaptic receptors and functions, conveys an extensive panoply of emerging morphology and electrophysiology. The taste system is not quiescent or passive in the embryo but is poised to respond to, and be shaped by, chemicals in the amniotic fluid which the embryo swallows (Bradley and Mistretta, 1973; Teicher and Blass, 1977; Bayol et al., 2007). In turn this active, developing, embryonic taste system is set for further extensive postnatal development as the newborn experiences a maternal diet via lactation and eventually weans to forage on its own. There is ample opportunity for chemicals in the diet to alter taste responses as this highly plastic system continues to add taste buds, receptors, afferents and central structures postnatally, after the embryonic taste system initiates considerable and potentially complex synaptic action.

4. Experimental Procedure

4.1. Preparation of brainstem slices

Sprague-Dawley rats at embryonic age (E) 14, 16, 18 and 20 days were used in this study. All procedures were carried out under National Institutes of Health and University of Michigan Animal Care and Use Committee approved protocols. Embryos were obtained from timed pregnant dams (Charles River) by hysterectomy under halothane anesthesia. The day on which a vaginal plug was found was considered to be E0 (Altman and Beyer, 1982, define sperm positive as day E1. When quoting the data from Altman and Beyer we have adjusted the embryonic timing to be consistent with the current investigation). Embryos were decapitated and the brain rapidly removed and cooled for 5 – 8 min in a 4°C oxygenated solution in which NaCl was replaced with isosmotic sucrose (Aghajanian and Rasmussen, 1989). The brainstem was blocked, embedded in agarose, secured to a Vibratome stage (Technical Products International) and sectioned horizontally into 225 μm-thick slices. Slices were incubated for at least 1 hour in oxygenated artificial cerebrospinal fluid (ACSF) at room temperature before a recording. ACSF contained (in mM) 124 NaCl, 5 KCl, 2.5 $CaCl_2$, 1.3 $MgSO_4$, 26 $NaHCO_3$, 1.25 NaH_2PO_4 and 25 dextrose, was gassed with a 95% O_2-5% CO_2 mixture to achieve a solution pH of 7.4.

4.2. Recording

Brainstem slices were transferred to a recording chamber attached to the stage of a fixed stage microscope (E600FN, Nikon). During recording, the slice was superfused at 2 – 2.5 ml/min with oxygenated ACSF. The recording chamber was kept at 32°C by a heating unit. Neurons were observed using infrared differential interface contrast optics (IR-DIC, Dodt and Zieglg nsberger, 1990) via a CCD camera (IR-1000, DAGE-MTI). Neurons were recorded in whole-cell configuration using a patch-clamp amplifier (AxoClamp 2B, Axon Instrument).

Borosilicate glass patch pipettes (TW150F-4, World Precision Instruments) were made using a two-stage puller (PP-83, Narishige) and filled with a solution that contained (in mM) 130 K-gluconate, 10 n-2-hydroxy-ethylpiperazine-*N'*-2 ethanesulfonic acid (HEPES), 10 ethylene glycol-bis(β-aminoethyl ether)-*N',N',N',N'*-tetraacetic acid (EGTA), 1 $MgCl_2$, 1 $CaCl_2$, and 2 ATP, buffered to pH 7.2 with KOH. Lucifer yellow (Sigma) was dissolved in the pipette solution at a concentration of 0.1% to label recorded neurons. Tip resistance of filled pipettes was 6–8 MΩ.

Neural responses to GABA, glutamate and glycine receptor agonists were recorded in current-clamp mode in the presence of voltage-gated Na^+ channel blocker tetrodotoxin (1 μM) and voltage-gated Ca^{2+} channel blocker $CdCl_2$ (200 μM) to isolate recorded neurons from synaptic input. Changes in neuronal input resistance were monitored by injecting negative constant current pulses (100 ms, 0.1 nA) into the neuron at a frequency of 0.15 Hz. The concentrations used were based on our earlier studies in adult rNST (Wang and Bradley, 1995).

To evoke postsynaptic currents (PSCs) or potentials (PSPs) in rNST neurons at E16, E18 and E20, a bipolar electrode (125 μm outer diameter; FHC) was carefully positioned on the ST and current stimuli (< 1 mA, 0.2 ms duration) delivered by a square pulse stimulator (S88, Grass Technologies). The stimulating site was separated from the recording site by approximately 200 – 300 μm. Glutamate- or GABA-receptor antagonists were used to confirm that the response initiated by the current stimulus was a postsynaptic response, and not evoked by direct current stimulation. The amplitude of the evoked excitatory postsynaptic currents (EPSCs) and EPSPs were maintained below action potential threshold by stimulus current intensity adjustment. EPSCs were recorded in voltage-clamp mode when

neurons were clamped at −70 mV. EPSPs and IPSPs were recorded in current-clamp mode when baseline membrane potential (V_m) was maintained at −70 mV and −30 mV by constant DC current respectively.

4.3. Confirmation of recording site

As described in our previous study (Suwabe et al., 2011) the ST was used as an anatomical landmark to locate the prenatal rNST in brainstem slices. After recording, patch pipettes were withdrawn from the neurons and the slices superfused with ACSF for approximately 15 min. Slices were then fixed in 4% paraformaldehyde and incubated in a blocking reagent containing 10% normal goat serum. Antibodies to rabbit polyclonal anti-calbindin D-28K (Chemicon) and mouse monoclonal anti-neurofilament (Sigma) were used to locate neurons and nerve fibers in the ST. The fixed slices were incubated in primary antibody at 4°C and after rinsing were incubated in secondary antibodies (Alexa Fluor 568-conjugated goat anti-rabbit or mouse IgG, Invitrogen). DAPI was used for nuclear staining. Slices were mounted on glass slides and coverslipped with an aqueous mounting medium (Fluoro-Gel, Electron Microscopy Sciences).

Confocal image stacks of the slices were acquired using a laser-scanning confocal microscope (Nikon C-1) and image acquisition software (EZ-C1, Nikon). Merged images were prepared from the confocal stacks using EZ-C1 software. Final images were enhanced only for brightness and contrast using Photoshop (Adobe).

4.4. Data analysis

Electrophysiological data were analyzed using the data analysis module Clampfit of pCLAMP 8 (Axon Instrument). The junction potential due to potassium gluconate (10 mV) was subtracted from V_m values. Whole-cell configuration was first established in current-clamp recording mode and resting membrane potential (V_{rest}), input resistance (R_{input}) and membrane time constant were measured. R_{input} was calculated from change in V_m evoked by a hyperpolarizing current (10 pA, 2 s long). Membrane time constant was measured by fitting a single exponential function to the data points in the hyperpolarizing phase of the same recording. Membrane capacitance was calculated by dividing the time constant by R_{input}.

Because our preliminary data showed there was no significant difference in amplitude of evoked PSP among E16, E18 and E20 rats (6 ± 2 mV, 8 ± 2 mV and 11 ± 2 mV, respectively; $n = 6$ each, $p > 0.1$, ANOVA), we did not compare characteristics between age groups in experiments on postsynaptic response as well as receptor expression.

Statistical analysis was conducted using PASW Statistics 18 (SPSS) software. Effects of Mg^{2+}-free solution and APV on EPSP amplitude were assessed using Kruskal–Wallis test followed by multiple Mann-Whitney tests with the Bonferroni correction. Significance level was set at 0.05. The results are expressed as median ± median absolute deviation; the other statistic values in the text mean ± SEM. Only responding neurons were included in statistical analysis.

Acknowledgments

Supported by National Institute on Deafness and Other Communication Disorders Grant number DC009982.

References

Aghajanian GK, Rasmussen K. Intracellular studies in the facial nucleus illustrating a simple new method for obtaining viable motoneurons in adult rat brain slices. Synapse. 1989; 3:331–338. [PubMed: 2740992]

Al-Ghoul WM, Miller MW. Development of the principal sensory nucleus of the trigeminal nerve of the rat and evidence for a transient synaptic field in the trigeminal sensory tract. J Comp Neurol. 1993; 330:476–490. [PubMed: 8391550]

Altman J, Bayer S. Development of the cranial nerve ganglia and related nuclei in the rat. Adv Anat Embryol Cell Biol. 1982; 74:1–90. [PubMed: 7090875]

Altman J, Bayer SA. Development of the brain stem in the rat. I. Thymidine-radiographic study of the time of origin of neurons of the lower medulla. J Comp Neurol. 1980; 194:1–35. [PubMed: 7440792]

Balland B, Lachamp P, Strube C, Kessler JP, Tell F. Glutamatergic synapses in the rat nucleus tractus solitarii develop by direct insertion of calcium-impermeable AMPA receptors and without activation of NMDA receptors. J Physiol. 2006; 574:245–261. [PubMed: 16690712]

Batten TFC, Pow DV, Saha S. Co-localisation of markers for glycinergic and GABAergic neurones in rat nucleus of the solitary tract: Implications for co-transmission. J Chem Neuroanat. 2010; 40:160–176. [PubMed: 20434539]

Bayol SA, Farrington SJ, Stickland NC. A maternal ‘junk food’ diet in pregnancy and lactation promotes an exacerbated taste for ’junk food’ and a greater propensity for obesity in rat offspring. Brit J Nutr. 2007; 98:843–851. [PubMed: 17697422]

Behar TN, Li YX, Tran HT, Ma W, Dunlap V, Scott C, Barker JL. GABA stimulates chemotaxis and chemokinesis of embryonic cortical neurons via calcium-dependent mechanisms. J Neurosci. 1966; 16:1808–1818. [PubMed: 8774448]

Bormann J, Feigenspan A. $GABA_C$ receptors. Trends Neurosci. 1995; 18:515–519. [PubMed: 8638289]

Bradley RM, Mistretta CM. Swallowing in fetal sheep. Science. 1973; 179:1016–1017. [PubMed: 4687587]

Brining SK, Smith DV. Distribution and synaptology of glossopharyngeal afferent nerve terminals in the nucleus of the solitary tract of the hamster. J Comp Neurol. 1996; 365:556–574. [PubMed: 8742302]

Demarque M, Represa A, Becq H, Khalilov I, Ben-Ari Y, Aniksztejn L. Paracrine intercellular communication by a Ca^{2+}- and SNARE-independent release of GABA and glutamate prior to synapse formation. Neuron. 2002; 36:1051–1061. [PubMed: 12495621]

Dodt H-U, Zieglgänsberger W. Visualizing unstained neurons in living brain slices by infrared DIC-videomicroscopy. Brain Res. 1990; 537:333–336. [PubMed: 2085783]

Du J, Bradley RM. Effect of GABA on acutely isolated neurons from the gustatory zone of the rat nucleus of the solitary tract. Chem Senses. 1998; 23:683–688. [PubMed: 9915114]

Dufour A, Tell F, Baude A. Perinatal development of inhibitory synapses in the nucleus tractus solitarii of the rat. Eur J Neurosci. 2010a; 32:538–549. [PubMed: 20718854]

Dufour A, Tell F, Kessler JP, Baude A. Mixed GABA-glycine synapses delineate a specific topography in the nucleus tractus solitarii of adult rat. J Physiol. 2010b; 588:1097–1115. [PubMed: 20156844]

Grabauskas G, Bradley RM. Postnatal development of inhibitory synaptic transmission in the rostral nucleus of the solitary tract. J Neurophysiol. 2001; 85:2203–2212. [PubMed: 11353035]

Heck N, Kilb W, Reiprich P, Kubota H, Furukawa T, Fukuda A, Luhmann HJ. GABA-A receptors regulate neocortical neuronal migration In vitro and in vivo. Cereb Cortex. 2007; 17:138–148. [PubMed: 16452638]

Herrmann K, Shatz CJ. Blockade of action potential activity alters initial arborization of thalamic axons within cortical layer 4. Proc Natl Acad Sci USA. 1995; 92:11244–11248. [PubMed: 7479973]

Hill DL. Development of taste responses in the rat parabrachial nucleus. J Neurophysiol. 1987; 57:481–495. [PubMed: 3559689]

Hill DL, Bradley RM, Mistretta CM. Development of taste responses in rat nucleus of solitary tract. J Neurophysiol. 1983; 50:879–895. [PubMed: 6631468]

Hill, DL.; May, OL. Development and plasticity of the gustatory portion of nucleus of the solitary tract. In: Bradley, RM., editor. The Role of the Nucleus of the Solitary Tract in Gustatory Processing. CRC Press; Boca Raton: 2006. p. 108-135.

Hill DL, Mistretta CM, Bradley RM. Developmental changes in taste response characteristics of rat single chorda tympani fibers. J Neurosci. 1982; 2:782–790. [PubMed: 7086483]

Hirai K, Yoshioka H, Kihara M, Hasegawa K, Sakamoto T, Sawada T, Fushiki S. Inhibiting neuronal migration by blocking NMDA receptors in the embryonic rat cerebral cortex: a tissue culture study. Develop Brain Res. 1999; 114:63–67.

Iwasato T, Erzurumlu RS, Huerta PT, Chen DF, Sasaoka T, Ulupinar E, Tonegawa S. NMDA receptor-dependent refinement of somatotopic maps. Neuron. 1997; 19:1201–1210. [PubMed: 9427244]

Katz LC, Shatz CJ. Synaptic activity and the construction of cortical circuits. Science. 1996; 274:1133–1138. [PubMed: 8895456]

Kihara M, Yoshioka H, Hirai K, Hasegawa K, Kizaki Z, Sawada T. Stimulation of N-methyl--aspartate (NMDA) receptors inhibits neuronal migration in embryonic cerebral cortex: a tissue culture study. Dev Brain Res. 2002; 138:195–198. [PubMed: 12354647]

King CT, Hill DL. Neuroanatomical alterations in the rat nucleus of the solitary tract following early maternal NaCl deprivation and subsequent NaCl repletion. J Comp Neurol. 1993; 333:531–542. [PubMed: 8370815]

King, MS. Anatomy of the rostral nucleus of the solitary tract. In: Bradley, RM., editor. The Role of the Nucleus of the Solitary tract in Gustatory Processing. CRC Press; Boca Raton: 2006. p. 17-38.

Komuro H, Rakic P. Modulation of neuronal migration by NMDA receptors. Science. 1993; 260:95–97. [PubMed: 8096653]

Lachamp P, Tell F, Kessler JP. Successive episodes of synapses production in the developing rat nucleus tractus solitarii. J Neurobiol. 2001; 52:336–342. [PubMed: 12210100]

Lasiter PS, Kachele DL. Postnatal development of the parabrachial gustatory zone in rat: dendritic morphology and mitochondrial enzyme activity. Brain Res Bull. 1988; 21:79–94. [PubMed: 2464423]

Lasiter PS, Wong DM, Kachele DL. Postnatal development of the rostral solitary nucleus in rat: Dendritic morphology and mitochondrial enzyme activity. Brain Res Bull. 1989; 22:313–321. [PubMed: 2468401]

Li CS, Smith DV. Glutamate receptor antagonists block gustatory afferent input to the nucleus of the solitary tract. J Neurophysiol. 1997; 77:1514–1525. [PubMed: 9084616]

Li Y, Erzurumlu RS, Chen C, Jhaveri S, Tonegawa S. Whisker-related neuronal patterns fail to develop in the trigeminal brainstem nuclei of NMDAR1 knockout mice. Cell. 1994; 76:427–437. [PubMed: 8313466]

Manent JB, Represa A. Neurotransmitters and brain maturation: early paracrine actions of GABA and glutamate modulate neuronal migration. Neuroscientist. 2007; 13:268–279. [PubMed: 17519369]

Mangold JE, Hill DL. Extensive reorganization of primary afferent projections into gustatory brainstem induced by feeding a sodium restricted diet during development: less is more. J Neurosci. 2007; 27:4650–4662. [PubMed: 17460078]

May OL, Erisir A, Hill DL. Modifications of gustatory nerve synapses onto nucleus of the solitary tract neurons induced by dietary sodium-restriction during development. J Comp Neurol. 2008; 508:529–541. [PubMed: 18366062]

Mistretta, CM.; Bradley, RM. Development of the sense of taste. In: Blass, EM., editor. Handbook of Behavioral Neurobiology. Vol. 8. Plenum Press; New York: 1985. p. 205-236.

Momose-Sato Y, Honda Y, Sasaki H, Sato K. Optical mapping of the functional organization of the rat trigeminal nucleus: Initial expression and spatiotemporal dynamics of sensory information transfer during embryogenesis. J Neurosci. 2004; 24:1366–1376. [PubMed: 14960608]

Nguyen L, Rigo JM, Rocher V, Belachew S, Malgrange B, Rogister B, Leprince P, Moonen G. Neurotransmitters as early signals for central nervous system development. Cell Tissue Res. 2001; 305:187–202. [PubMed: 11545256]

Rampon C, Luppi PH, Fort P, Peyron C, Jouvet M. Distribution of glycine-immunoreactive cell bodies and fibers in the rat brain. Neuroscience. 1996; 75:737–755. [PubMed: 8951870]

Rao HW, Pio J, Kessler JP. Postnatal development of synaptophysin immunoreactivity in the rat nucleus tractus solitarii and caudal ventrolateral medulla. Dev Brain Res. 1999; 112:281–285. [PubMed: 9878786]

Sato K, Momose-Sato Y, Hirota A, Sakai T, Kamino K. Optical mapping of neural responses in the embryonic rat brainstem with reference to the early functional organization of vagal nuclei. J Neurosci. 1998; 18:1345–1362. [PubMed: 9454844]

Schlaggar BL, Fox K, O'Leary DM. Postsynaptic control of plasticity in developing somatosensory cortex. Nature. 1993; 364:623–626. [PubMed: 8102476]

Shatz CJ, Stryker MP. Prenatal tetrodotoxin infusion blocks segregation of retinogeniculate afferents. Science. 1988; 242:87–89. [PubMed: 3175636]

Smith, DV.; Lemon, CH. Neural coding in the rNST. In: Bradley, RM., editor. The Role of the Nucleus of the Solitary Tract in Gustatory Processing. CRC Press; Boca Raton: 2006. p. 83-105.

Sretavan DW, Shatz CJ, Stryker MP. Modification of retinal ganglion cell axon morphology by prenatal infusion of tetrodotoxin. Nature. 1988; 336:468–471. [PubMed: 2461517]

Suwabe T, Mistretta CM, Krull CE, Bradley RM. Pre and postnatal differences in membrane, action potential and ion channel properties of rostral nucleus of the solitary tract neurons. J Neurophysiol. 2011; 106:2709–2719. [PubMed: 21865434]

Teicher MH, Blass EM. First suckling response of the newborn albino rat: the roles of olfaction and amniotic fluid. Science. 1977; 198:635–636. [PubMed: 918660]

Vincent A, Tell F. Postnatal development of rat nucleus tractus solitarius neurons: Morphological and electrophysiological evidence. Neuroscience. 1999; 93:293–305. [PubMed: 10430493]

Vogt MB, Hill DL. Enduring alterations in neurophysiological taste responses after early dietary sodium deprivation. J Neurophysiol. 1993; 69:832–841. [PubMed: 8385197]

Wang L, Bradley RM. In vitro study of afferent synaptic transmission in the rostral gustatory zone of the rat nucleus of the solitary tract. Brain Res. 1995; 702:188–198. [PubMed: 8846076]

Wang L, Bradley RM. Influence of GABA on neurons of the gustatory zone of the rat nucleus of the solitary tract. Brain Res. 1993; 616:144–153. [PubMed: 8358606]

Whitehead MC. Anatomy of the gustatory system in the hamster: synaptology of facial afferent terminals in the solitary nucleus. J Comp Neurol. 1986; 244:72–85. [PubMed: 3950091]

Yoshioka M, Tashiro Y, Inoue K, Kawai Y. Postnatal development of GABAergic axon terminals in the rat nucleus of tractus solitarius. Brain Res. 2006; 1107:111–120. [PubMed: 16828714]

Zafra F, Aragón C, Olivares L, Danbolt NC, Giménez C, Storm-Mathisen J. Glycine transporters are differentially expressed among CNS cells. J Neurosci. 1995; 15:3952–3969. [PubMed: 7751957]

Zhang LL, Ashwell KWS. The development of cranial nerve and visceral afferents to the nucleus of the solitary tract in the rat. Anat Embryol. 2001a; 204:135–151. [PubMed: 11556529]

Zhang LL, Ashwell KWS. Development of the cyto- and chemoarchitectural organization of the rat nucleus of the solitary tract. Anat Embryol. 2001b; 203:265–282. [PubMed: 11396854]

Highlights

We detail development of excitation and inhibition in rat brainstem gustatory nucleus.

We demonstrate appearance of glutamate, GABA and glycine receptors as early as E14.

We analyze development of rNST synaptic responses to solitary tract stimulation.

The underlying mechanisms of developing synaptic activity are explored.

We correlate functional and anatomical development rNST synapses.

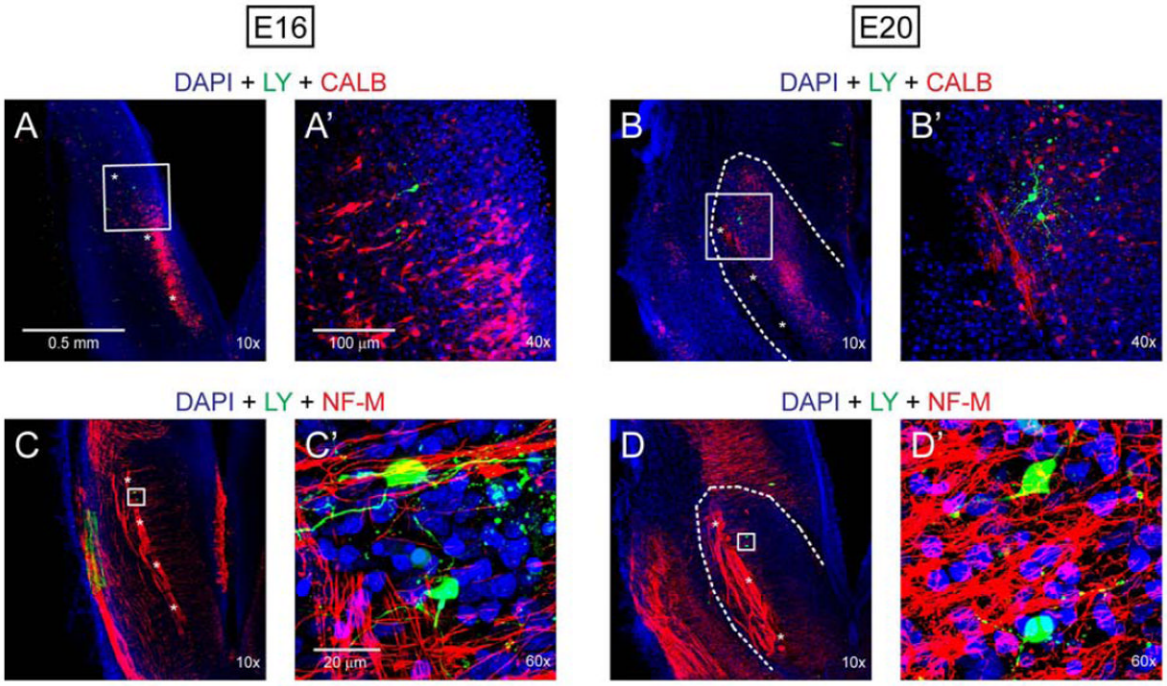

Fig. 1.

Post-recording immunohistochemistry in E16 and E20 brainstem slices. Recorded neurons (green) were intracellularly labeled by Lucifer yellow (LY). *A, A', B and B'*: Recorded neurons were located in a cluster of calbindin (CALB)-immunoreactive cells (red) surrounding ST (indicated by asterisks). *C, C', D and D'*: ST and the fibers extending medially to presumptive NST were neurofilament (NF-M)- immunoreactive (red). Recorded neurons were located in a meshwork of the NF-M-immunoreactive fibers. Blue color in all images was derived from nuclear staining with DAPI.

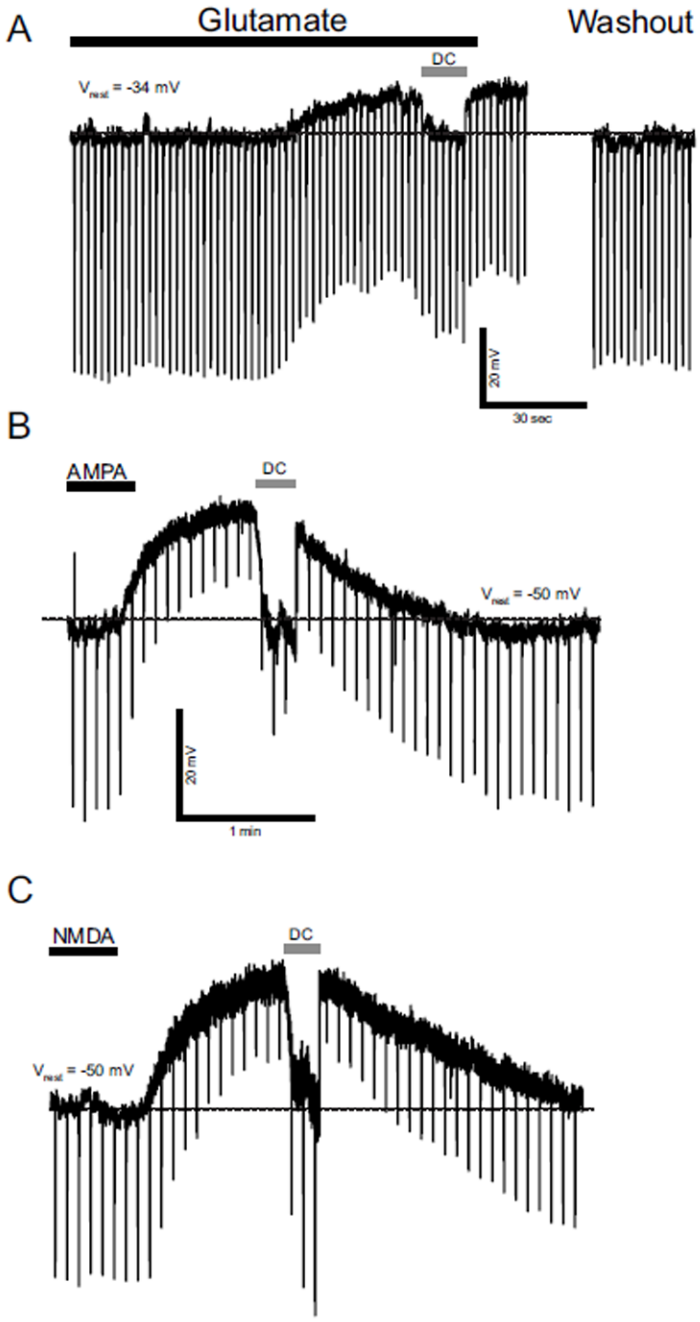

Fig. 2.

A: Responses to glutamate, E14 neuron. This neuron responded to 0.5 mM glutamate with depolarization. Hyperpolarizing current pulses were injected to monitor change in R_{input}. V_m was restored to V_{rest} level (dashed line) with constant DC current (DC) for calculation of change in R_{input}. In this neuron, glutamate decreased R_{input}. *B* and *C*: Response to glutamate receptor agonists NMDA and AMPA, E20 rNST neuron. This neuron responded to (*B*) 10 μM AMPA and (*C*) 100 μM NMDA with membrane depolarization. AMPA and NMDA decreased and increased R_{input} respectively. Black bars above traces indicate timing and duration of the drug application. Dashed lines indicate V_{rest} level.

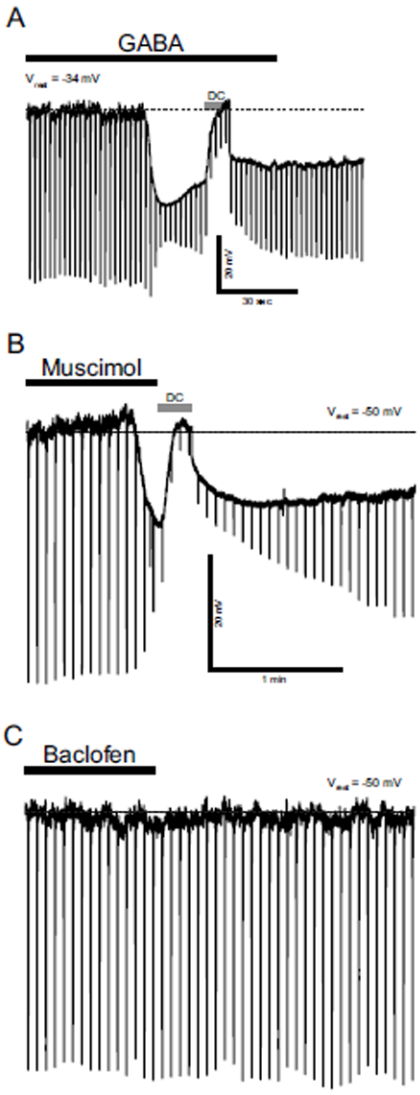

Fig. 3.

A: Responses to GABA, E14 neuron. This neuron responded to 0.5 mM GABA with hyperpolarization. Hyperpolarizing current pulses were injected to monitor change in R_{input}. V_m was restored to V_{rest} level (dashed line) with constant DC current (DC) for calculation of change in R_{input}. *B* and *C*: Response of an rNST neuron to the $GABA_A$ receptor agonist, Muscimol, and $GABA_B$ receptor agonist, Baclofen, at E16. This neuron responded to 10 μM muscimol with membrane hyperpolarization and decrease in R_{input} (*B*) whereas it did not show significant response to100 μM baclofen (*C*).

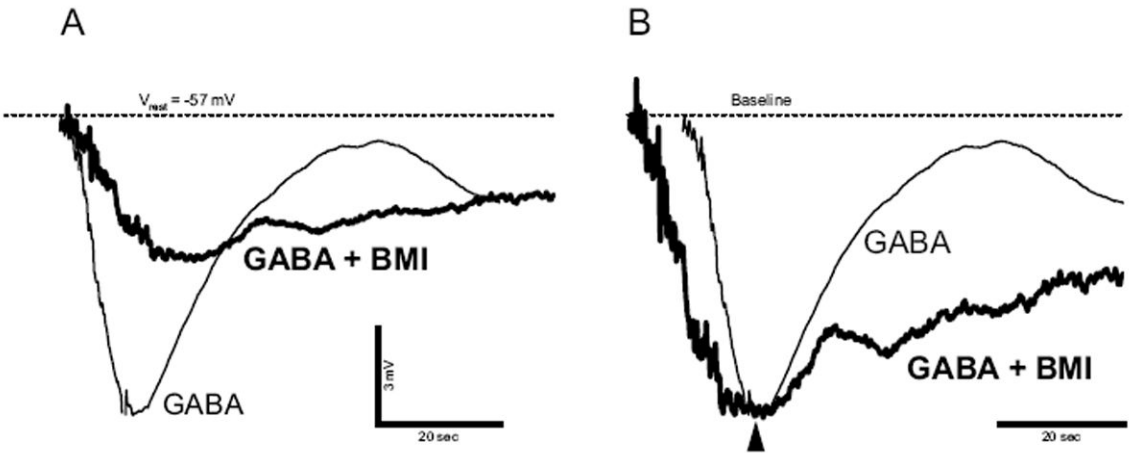

Fig. 4.

GABA-induced hyperpolarization is insensitive to the $GABA_A$ receptor antagonist bicuculline (BMI), E20 neuron. *A*: GABA-induced hyperpolarizations in absence (thin-lined trace) and presence (thick-lined trace) of 200 μM BMI. *B*: Comparison of the decay between GABA-induced hyperpolarizations in absence (thin-lined trace) and presence (thick-lined trace) of BMI. The hyperpolarizations were scaled so that those peaks superimposed. Dashed line indicates V_{rest} level.

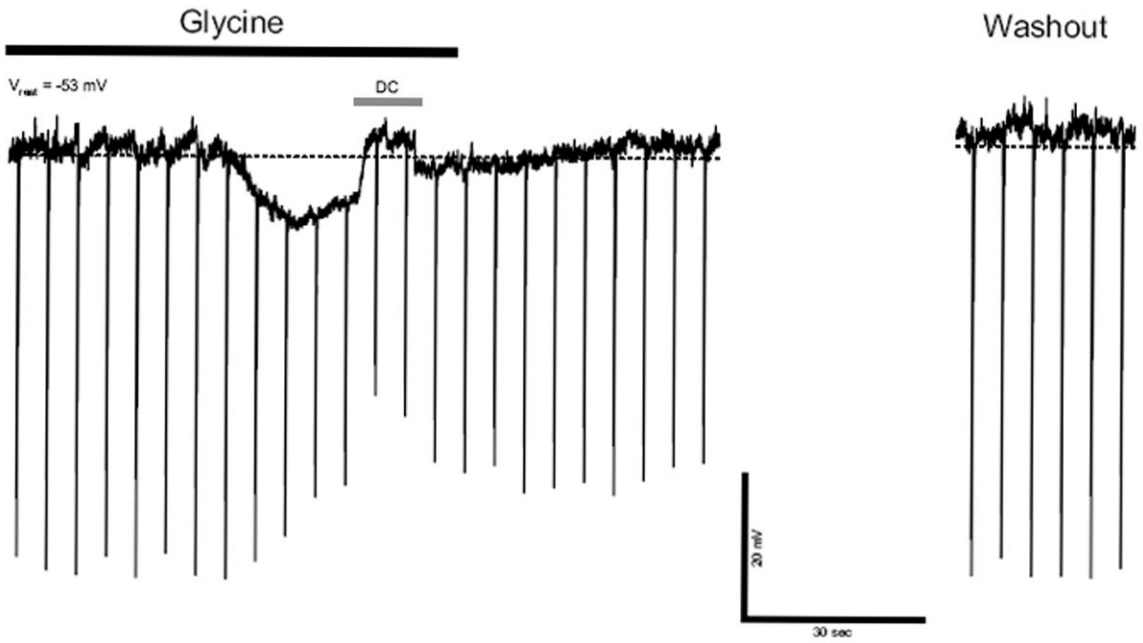

Fig. 5.
Response to glycine in an E16 neuron. This neuron responded to 1 mM glycine with membrane hyperpolarization and reduction of R_{input}.

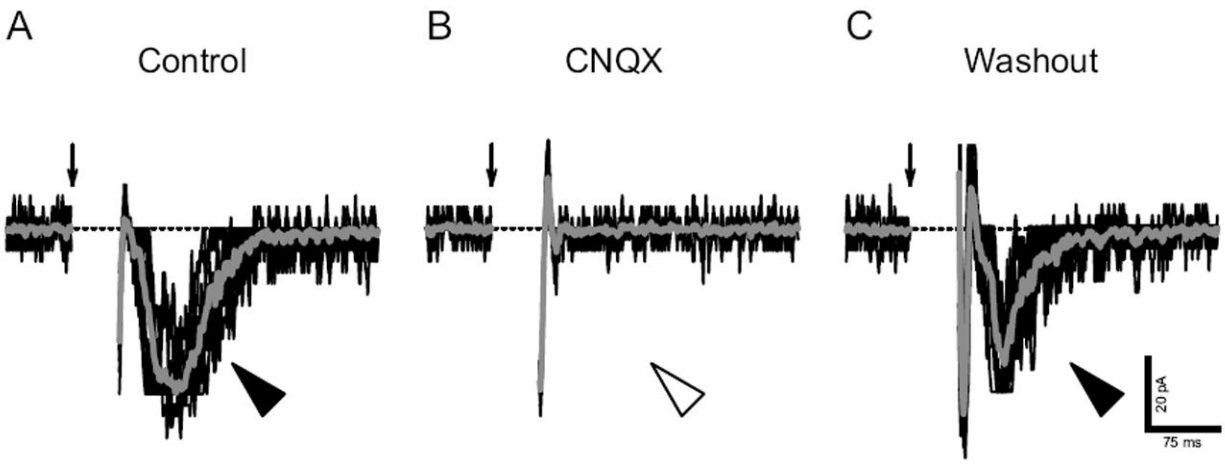

Fig. 6.

Excitatory postsynaptic currents (EPSCs) evoked by current stimuli to ST in an E16 neuron. *A*: EPSCs (filled arrowhead). *B*: The AMPA/kainate-type receptor antagonist CNQX eliminated the EPSCs (open arrow). *C*: The EPSCs reappeared after the washout of CNQX. EPSCs were evoked by current stimuli repeated at 0.1 Hz (one stimulus per trial). Gray traces show the average of individual trials (black traces). Arrows point out stimulus onsets. Dashed lines indicate 0 pA level. Holding potential was set at -70 mV.

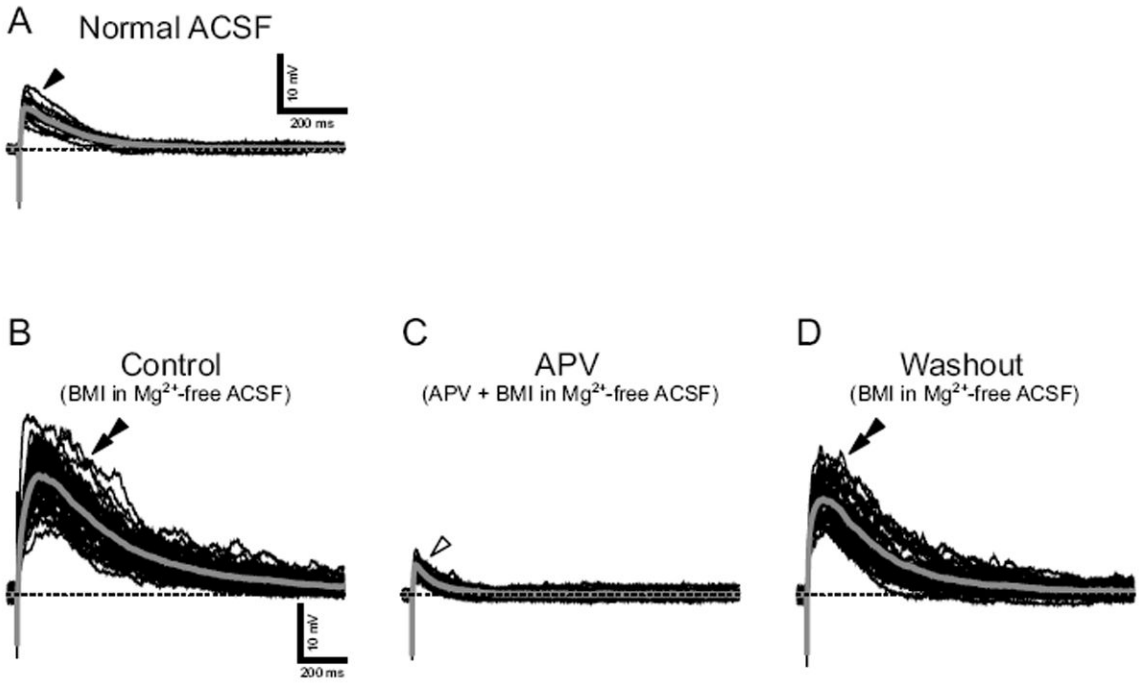

Fig. 7.

NMDA receptor-mediated excitatory postsynaptic potentials (EPSPs) evoked by current stimuli to ST in an E20 neuron. *A*: EPSPs in normal ACSF (filled arrowhead). *B*: The EPSPs enlarged in Mg^{2+}-free ACSF (double arrowhead). *C*: The enlarged EPSPs were suppressed by a NMDA-type receptor antagonist APV (open arrowhead). *D*: The enlarged EPSPs reappeared after the washout of APV (double arrowhead). EPSPs were evoked by current stimuli repeated at 0.1 Hz. Baseline V_m was maintained at -70 mV (dash lines) with constant DC current.

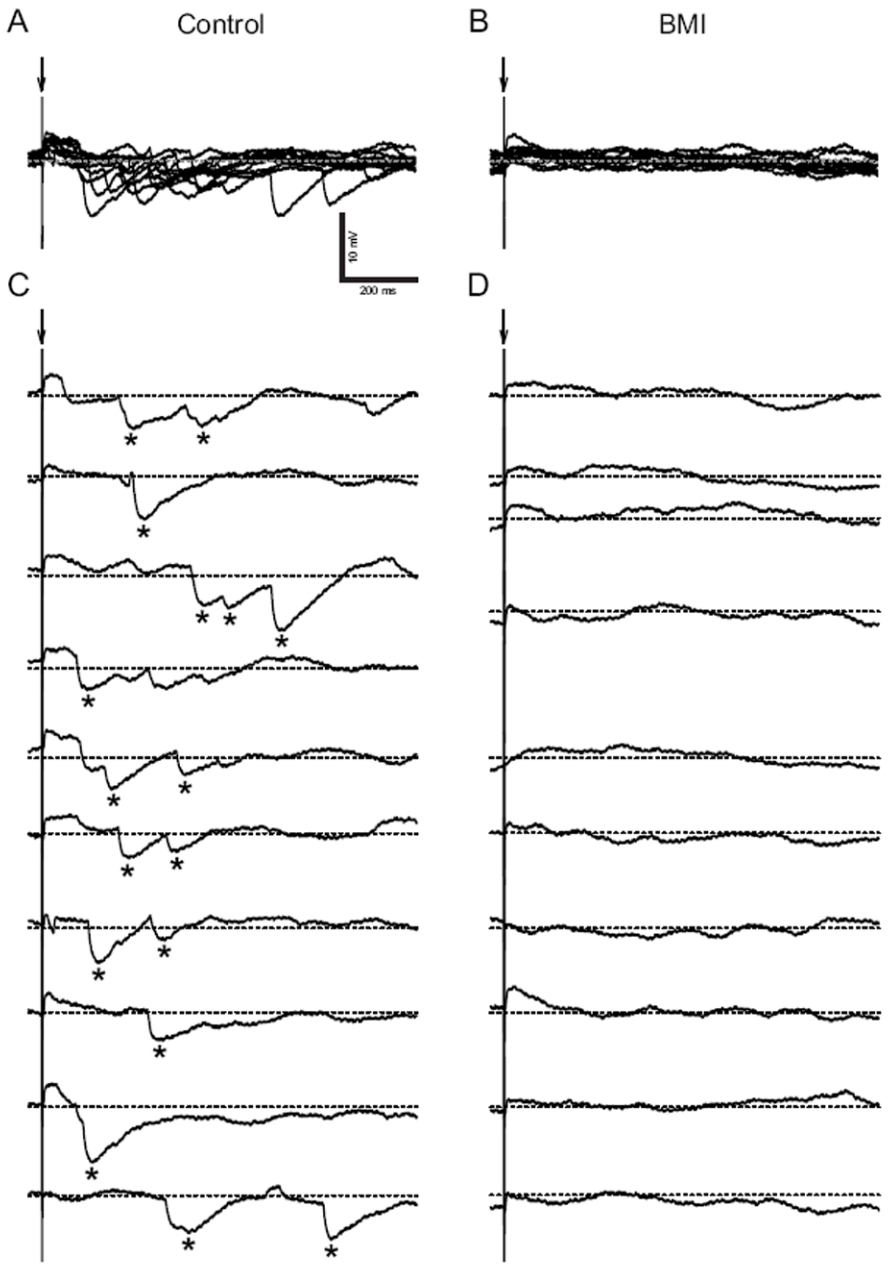

Fig. 8.

Inhibitory postsynaptic potentials (IPSPs) evoked by current stimuli to ST in an E20 neuron. *A* and *B*, superimposed series of evoked IPSPs before and after BMI application. *A*: Evoked IPSPs (asterisks). *B*: The IPSPs were eliminated by BMI. IPSPs were evoked by current stimuli repeated at 0.1 Hz. Baseline V_m was maintained at -30 mV (dash lines) with constant DC current. *C* and *D*, individual traces of evoked IPSPs before and after BMI application. *C*: The onset time of IPSPs varied from trial to trial. Single stimulations evoke both single and multiple IPSPs as indicated by asterisks.

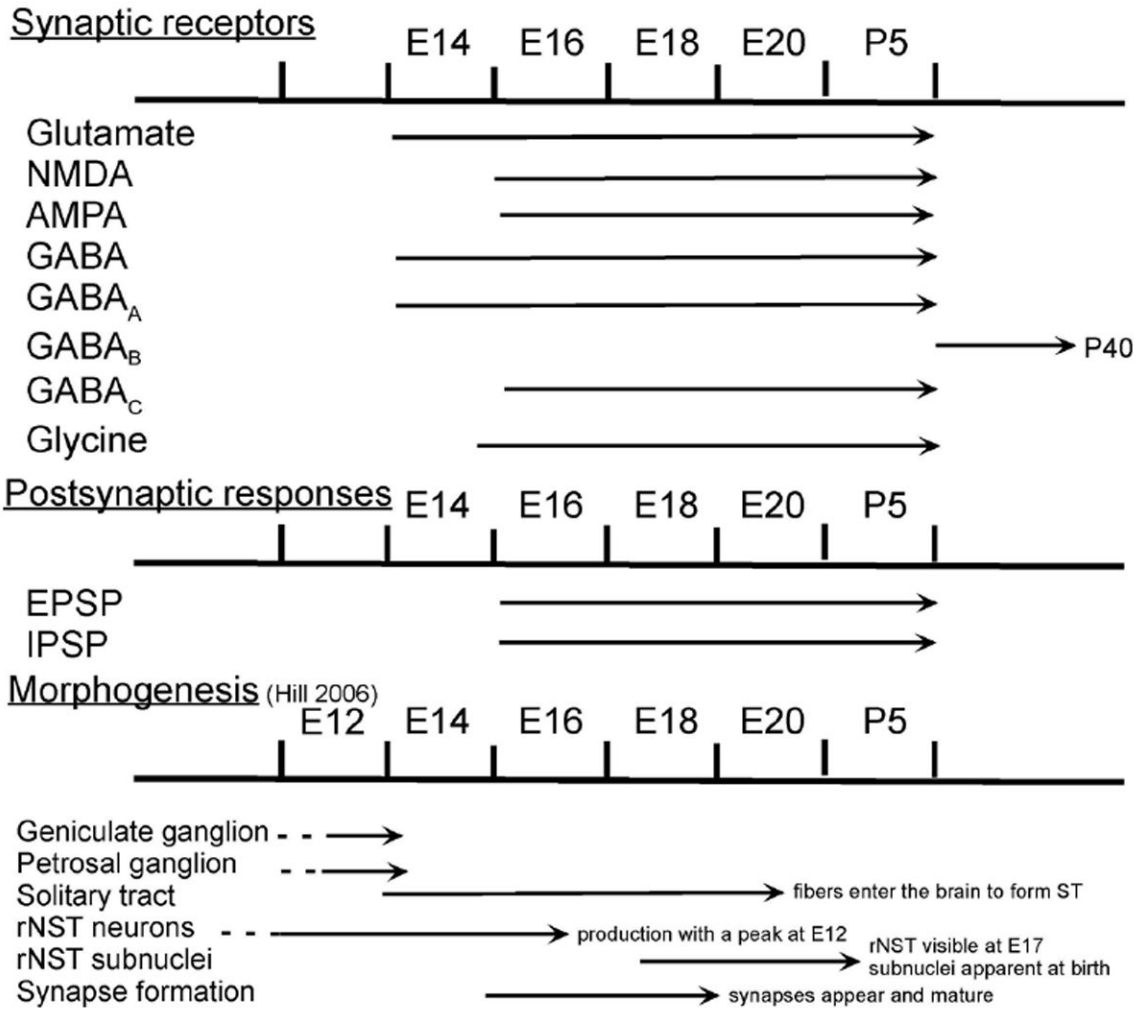

Fig. 9.

Timelines of the prenatal development of the rNST including synaptic receptor expression and postsynaptic potentials evoked by ST stimulation. Current knowledge of morphological events in rNST embryogenesis (Hill, 2006) is also included to provide correlations between structural and functional developments. (The rodent trigeminal sensory nucleus undergoes a similar developmental time line (see Fig. 12 in Momose-Sato, 2004)